Theory and Applications of Formation Control in a Perceptive Referenced Frame *

W. Kang
Mathematics Department
Naval Postgraduate School
Monterey, CA 93943

N. Xi
Department of ECE
Michigan State University
East Lansing, MI 48824

Andy Sparks
AFRL/VAAD, Bldg 146,
Wright-Patterson AFB
WPAFB, OH 45433

Abstract

A general method of controller design is developed in this paper for the purpose of formation keeping and reconfiguration of multiple autonomous vehicles. Controllers are designed to keep multiple vehicles in a required formation, and to coordinate the vehicles in the presence of environmental changes. The method is applicable to a large variety of autonomous agents. Examples and simulations are given for ground vehicles, robotic arms and satellites.

1 Introduction

In this paper, a general method of controller design is developed for the formation of multiple autonomous vehicles. Using the design method, controllers can be found to keep multiple vehicles in a required formation, and to coordinate the vehicles in the presence of environmental changes. In this study, the model adopted for autonomous vehicles is a general dynamical system of ordinary differential equations. Examples are given in this paper to illustrate the applications of the method to ground vehicle formations, robotic arm formatons and satellite constellations.

The controllers developed in this paper are fundamentally different from the existing centralized or decentralized controllers. The feedback for each individual vehicle is designed separately using any classical feedback design algorithm such as LQR or H_∞. Then, the separately designed feedbacks are coordinated through a set of action references, which play the role of a higher level controller. The advantage of separately design the feedback for each vehicle is that the feedbacks are not affected when vehicles are added into or removed from the formation. Since all local feedbacks share the same value of the action reference, the coordination among the vehicles can be achieved by suitably define the action reference. Several useful coordination strategies in the presence of unexpected event is discussed in section 3.

In section 2, the design method is summarized in a simple four-step algorithm. In section 3, several coordination strategies are studied for multiple ground vehicles, robot arms and satellites. Simulations and lab test are shown.

2 Formation and controller design

2.1 Formation structure and action reference

The model of a complex system with multiple subsystems (vehicles) is given by the following equations

$$\begin{aligned} &\frac{dx_i}{dt} = f_i(x_i, u_i, r_i), \;\; 1 \le i \le k \\ &y_i = h_i(x_i) \end{aligned} \tag{1}$$

where k is the total number of subsystems. The variable $x_i \in I\!R^{n_i}$ is the state of the ith subsystem. The function r_i represents the coupling of subsystems. It is a function of (x_j, u_j) for $j \neq i$. The input $u_i \in I\!R^{m_i}$ is the control variable for the ith subsystem. The output function $h_i(x_i)$ represents the performance. For instance, for the formation of multiple ground vehicles, h_i represents the position of the ith vehicle. For the formation of multiple robot manipulators moving an object, h_i represents the force exerted on the object and the position of the ith manipulator. We assume that $y_i \in I\!R^p$, where p is a constant for all subsystems.

A *formation* is defined in a coordinate frame, which moves with the desired trajectory. Let $y_d(s)$ be any curve in $I\!R^p$ with parameter s. Let $\mathcal{F}(s) = \left[\begin{array}{cccc} \mathbf{e}_1(s), & \mathbf{e}_2(s), & \cdots, \mathbf{e}_p(s) \end{array} \right]$ be p orthonormal vectors in $I\!R^p$ which forms a moving frame. The origin of the moving frame is $y_d(s)$. A formation consists of k points in $\mathcal{F}$, denoted by $F = \{P_1, P_2, \cdots, P_k\}$, where $P_i = \sum_{j=1}^{p} \alpha_{ij} \mathbf{e}_j$. In general, α_{ij} is a function of s or time t. The formation is time-variant.

The concept *action reference* is a key parameter determined by the task of a control problem. In the for-

*Research supported in part by NSF IRI 9796287, NSF IRI 9796300 and Air Force Research Lab.

mation control problem, a convenient choice for action reference is s, the parameter used for the desired path $y_d(s)$. How to compute the value of action reference using sensor information is discussed in § 4 using reference projections. The projection converts the sensory information into the value of the action reference, then the value of s is converted to the synthetic time which is used to coordinate the lower level feedbacks.

2.2 Control law design

In this section, we introduce the reference projection method of controller design for the formation control problem. The controller design using the reference projection method has the following four steps.

The first step is to generate the desired path for each subsystem in the formation. Given a desired path $y_d(s)$, and given a formation $\{P_1, \cdots, P_k\}$ in the moving frame $\mathcal{F}$, the path for each subsystem is generated by

$$y_{di}(s) = y_d(s) + \sum_{j=1}^{p} \alpha_{ij} \mathbf{e}_j(s) \tag{2}$$

The action reference is the parameter s. The speed of the formation moving along $y_d(s)$ is determined by the task. It is defined by a strictly increasing function

$$s = v(t).$$

A formation control law is a feedback $u = u(x)$ which satisfies

$$\lim_{t\to\infty} (y_i(t) - y_{di}(v(t))) = 0. \tag{3}$$

Furthermore, if the initial position is on the desired path, then the trajectory of the controlled system follows the path. More specifically, there exists an initial condition of the system $x_0 = (x_{01}, x_{02}, \cdots, x_{0k})^T$ such that the trajectory starting from x_0 satisfies $h_i(x(t)) = y_{di}(t)$. Denote this path by $x_{di}(s)$ or $x_{di}(v(t))$.

The second step in the controller design is to find control laws for subsystems. They might be time varying feedbacks. The control law $u_i = u_i(x,t)$, $1 \le i \le k$, for each subsystem is designed separately using any existing method of signal tracking or path following. Two subsystems may adopt different control design algorithms.

Theoretically, the control laws $u_i = u_i(x,t)$ can drive the system move in formation along y_d because they are designed to satisfy (3). However, the feedbacks are designed separately. There is no coordination between the subsystems. To improve the performance and coordination of the feedback, a projection mapping is introduced in the next step.

The third step is to define the *reference projection*. The projection is a transformation $s = \gamma(x)$ satisfying

$$\gamma(x_d(s)) = s \tag{4}$$

i.e. if the state is on the desired path, γ should give the corresponding value of s on the desired trajectory $x_d(s)$. For example, given any state x_0, let $x_d(s_0)$ be the orthogonal projection from x_0 to $x_d(s)$. If we define $\gamma(x_0) = s_0$, then it satisfies (4). However, orthogonal projection is not the only way to define γ. It is shown in section 4 that changing the projection transformation γ can fundamentally change the way subsystems coordinated with each other.

The last step of the controller design is to construct a non-time based feedback law, which is used to control the system of multiple vehicles. The process is simply a substitution. The control law is given by

$$u_i(x) = u_i(x, T(x)), \quad T(x) = v^{-1}(\gamma(x)) \tag{5}$$

Notice that the time t is replaced by the perceptive or synthetic time, $T(x) = v^{-1}(\gamma(x))$. The closed-loop system with non-time based feedback is $\dot{x}_i = f_i(x, u_i(x))$. Mission tasks and coordination requirements determine which reference projection to be adopted. How to defined a projection reflecting the coordination requirement of a mission is discussed in § 4.

3 Error Dynamics and Stability

Two error dynamics are derived in this section. The first error equation is under the time-variant feedback $u_i(x,t)$. The error dynamics is

$$\begin{array}{l} \dot{e}_i = E_i(e_i, t), \quad for\ i = 1, \cdots, k, \\ E_i(e_i, t) = f_i(e_i + x_{di}, u_i(e_i + x_{di}, t)) - f_i(x_{di}, u_i(x_{di}, t)), \\ e_i = x_i(t) - x_{di}(t) \end{array} \tag{6}$$

Under the non-time based feedback $u_i(x_i, T_i(x))$, the error dynamics is

$$\begin{array}{l} \dot{\bar{e}}_i = E_i(\bar{e}_i, T_i) - f_i(x_{di}(T_i), u_i(x_{di}(T_i), T_i))(\dot{T}_i(x) - 1), \\ \dot{x}_i = f_i(x_i, u_i(x_i, T_i(x))), \quad for\ i = 1, \cdots, k. \\ \bar{e}_i = x_i(t) - x_{di}(T_i), \end{array} \tag{7}$$

where $x = \left[\begin{array}{cccc} x_1 & x_2 & \cdots & x_k \end{array}\right]^T$.

The two errors e_i and $\bar{e}_i$ follows different dynamics. The stability of e_i does not automatically imply the stability of $\bar{e}_i$. The performance of $T(x)$ is critical for the stability of (7). In this paper, a δ neighborhood of $x_d(s)$ is the set of all x such that the distance from the point x to the curve x_d is less than δ. In this paper, we assume

Assumption A1: The vector fields and functions $f(x, u(x,t))$, $u(x,t)$, $\dfrac{\partial f}{\partial x}$, $\dfrac{\partial f}{\partial u}$, $\dfrac{\partial u}{\partial x}$, $\dfrac{\partial u}{\partial t}$, and $\dfrac{\partial T}{\partial x}$ are all bounded for $t > 0$ and for x in a δ neighborhood of x_d.

The nonlinear vector $f(x,t)$ represents the rate of change of the state variable. It is reasonable to require

in **A1** that the speed and acceleration of the state variables of a mechanical system are bounded around the desired path. **A1** also assumes that $u(x,t)$ and its derivatives are bound. It implies that the controller can react to the change of state and time at a limited rate.

Theorem 0.1 *Suppose (6) is uniformly exponentially stable in $||e|| < \delta$. Suppose $x_i = f_i(x_i, u_i(x_i, T_i(x)))$ has a solution and it satisfies $\dot{T}(x(t)) - \begin{bmatrix} 1 & 1 & \cdots & 1 \end{bmatrix}^T$ approaching zero uniformly and exponentially whenever $||\bar{e}(0)|| < \delta$. Then, there exists a $\delta_1 > 0$ so that $\lim_{t\to\infty} \bar{e}(t) = 0$ provided $||\bar{e}(0)|| < \delta_1$.*

Proof. From the converse theorem of stability, there exists a Lyapunov function $V_i(e_i, t)$ such that

$$\begin{array}{ll} \alpha_1||e_i||^2 \le V_i(e_i,t) \le \alpha_2||e_i||^2, & t \ge 0, \\ \left|\frac{\partial V_i}{\partial e_i}(e_i,t)\right| \le \alpha_3||e_i||, & t \ge 0, \\ \frac{\partial V_i}{\partial t} + \frac{\partial V_i}{\partial e_i}E(e_i,t) = -||e_i||^2, & t \ge 0. \end{array} \quad (8)$$

in a neighborhood $|e_i| < \delta$. Under the non-time based controller, the error is replaced by $\bar{e}_i$. The Lyapunov function for $\bar{e}_i$ is $V_i(\bar{e}_i, T(x))$. Define $V(\bar{e}, T) = \sum_{i=1}^k V_i(\bar{e}_i, T_i)$, where $\bar{e} = \begin{bmatrix} \bar{e}_1 & \bar{e}_2 & \cdots & \bar{e}_k \end{bmatrix}^T$. The derivative of $V(\bar{e}, T)$ in the direction of (7) is

$$\begin{array}{l} \dot{V}(\bar{e},T) = \frac{\partial V}{\partial T}\dot{T} + \frac{\partial V}{\partial \bar{e}}\bar{e} = -||\bar{e}||^2 \\ +\sum_{i=1}^k \left(\frac{\partial V_i}{\partial T_i} - \frac{\partial V_i}{\partial \bar{e}_i}f_i(x_{di}, u_i(x_{d1}, T_i))\right)(\dot{T}_i - 1) \end{array} \quad (9)$$

From **A1**, we know that $E(e,t)$ is bounded in $||e|| < \delta$. So, the equations in (8) imply that $\frac{\partial V}{\partial t}(e,t)$ is bounded in $0 \le t \le \infty$ and $||e|| \le \delta$. From the second equation of (8), it is known that $\frac{\partial V}{\partial e}(e,t)$ is also bounded for $||e_j|| < \delta$. Therefore,

$$\frac{\partial V_i}{\partial T_i}(\bar{e}_i, T_i) - \frac{\partial V_i}{\partial \bar{e}_i}(\bar{e}_i, T_i) f(x_{di}, u_i(x_{di}, T_i))$$

is bounded in $||\bar{e}|| \le \delta$. Since $\dot{T}_i(x) - 1$ is uniformly exponentially convergent to zero for all $1 \le i \le k$, there exists $M > 0$ and $\lambda > 0$ such that

$$\left(\frac{\partial V_i}{\partial T_i} - \frac{\partial V_i}{\partial \bar{e}_i}f_i(x_{di}, u_i(x_{di}, T_i))\right)(\dot{T}_i - 1) < Me^{-\lambda t}$$

for all $1 \le i \le k$, provided $||\bar{e}|| < \delta$. From (9),

$$\begin{array}{l} \dot{V}(\bar{e},T) < -||\bar{e}||^2 + kMe^{-\lambda t} \\ < -\frac{1}{\alpha_2}V(\bar{e},T) + kMe^{-\lambda t}, \quad ||\bar{e}|| < \delta. \end{array} \quad (10)$$

At any frozen time t_0, if $\bar{e}(t_0) < \delta$, then

$$\dot{V}(\bar{e},T) < -\frac{1}{\alpha_2}V(\bar{e},T) + kMe^{-\lambda t_0}e^{-\lambda(t-t_0)},$$

for $t > t_0$. This implies

$$\frac{d}{dt}\left(e^{\frac{1}{\alpha_2}(t-t_0)}V(\bar{e},T)\right) < kMe^{-\lambda t_0}e^{(-\lambda+\frac{1}{\alpha_2})(t-t_0)}.$$

Integrating the inequality over $[t_0, t]$ yields

$$\begin{array}{l} V(\bar{e},T) \le e^{-\frac{1}{\alpha_2}(t-t_0)}V(\bar{e}(t_0), T(x(t_0))) \\ +\frac{kMe^{-\lambda t_0}}{-\lambda+\alpha_2^{-1}}\left(e^{-\lambda(t-t_0)} - e^{-\frac{1}{\alpha_2}(t-t_0)}\right), \end{array} \quad (11)$$

provided $t \ge t_0$ and $||\bar{e}(t)|| < \delta$. There exists $t_0 > 0$ so that $\frac{kMe^{-\lambda t_0}}{-\lambda+\alpha_1^{-1}}\left(e^{-\lambda(t-t_0)} + e^{-\frac{1}{\alpha_2}(t-t_0)}\right) < \frac{\alpha_1}{2}\delta^2$, for $t \ge t_0$ and $||\bar{e}|| < \delta$. If $||\bar{e}(t_0)|| < \frac{\alpha_1}{2\alpha_2}\delta^2$, (8) and (11) imply

$$\begin{array}{l} \alpha_1||\bar{e}||^2 \le V(\bar{e},T) \le V(\bar{e}(t_0), T(x(t_0))) + \frac{\alpha_1}{2}\delta^2 \\ \le \alpha_2||\bar{e}(t_0)||^2 + \frac{\alpha_1}{2}\delta^2 \le \alpha_1\delta^2. \end{array}$$

Therefore, $||\bar{e}(t)|| \le \delta$ for all $t \ge t_0$, provided

$$||\bar{e}(t_0)|| < \frac{\alpha_1}{2\alpha_2}\delta^2. \quad (12)$$

Thus, (11) holds for $t \ge t_0$ if the initial error satisfies (12). From (11), it is easy to derive that $\lim_{t\to\infty} V(\bar{e},T) = 0$, provided (12) holds. Therefore, $\lim_{t\to\infty} \bar{e}(t) = 0$. Because the right side of (7) is uniformly bounded in $||\bar{e}|| < \delta$, there exists $\delta_1 > 0$ so that $||\bar{e}(0)|| < \delta_1$ implies (12). This proves that $\lim_{t\to\infty} \bar{e}(t) = 0$ if $||\bar{e}(0)|| < \delta_1$. ◁

4 Coordination using action reference and reference projection

In the following, we use several examples to illustrate how to select a reference projection to achieve the coordination requirement of the formation. Formations of different types of vehicles are studied in this section, including ground vehicles, robot arms and space satellites.

3.1 Movement with a leader

Using ground vehicles as an example. Suppose the desired path of the formation is the line $x_d = s, y = 0$. Suppose that $u_i(x,t)$ drives the ith vehicle along its desired path, and it keeps the vehicle in formation. Let's define the reference projection by $\gamma(x) = x_1$. Then, all the vehicles in the formation compute their perceptive time based on the location of the vehicle $i = 1$, which is called the leader. If the leader slows down or stops, the perceptive time of all other vehicles slows down and stop. It results in the slow down and stop of the entire formation.

3.2 Coordinated motion of dual robot

In the following, the method is applied to a system of multiple robot manipulators. Lab experiments are carried out for the formation of two robot arms carrying a box. The coordination task, shown as Figure 1, is

a special case of formation control. It can be expressed by the requirement that for any point along the path of the object, the states of the robots should be in the desired position with the desired contacting force. For given motion plans and desired contact forces of each individual robot ${r_i}^d(s)$ and ${f_i}^d(s)$, $i = 1, 2, ...k$, and the measurements $r_i,\ f_i,\ i = 1,\ 2, \ldots k$, define a coordination criterion

$$J = \sum_{i=1}^{k} \quad \Big[\left(r_i^d(s) - r_i\right)^T W_{r_i} \left(r_i^d(s) - r_i\right) + \left(f_i^d(s) - f_i\right)^T W_{f_i} \left(f_i^d(s) - f_i\right) \Big], \tag{13}$$

where, W_{r_i} and W_{f_i}, $i = 1,\ 2, \ldots k$ are weight matrices. They can weigh the coordination errors in the different directions to insure efficient coordinated control in some specific directions, which are determined by the task. The value of s is computed by the reference projection γ. Its value is the optimal motion reference s^* which solves the following optimization problem $\min_{s \in S}\ J$. The closed form solution can be easily obtained for most tasks such as straight lines , circles, etc., by solving

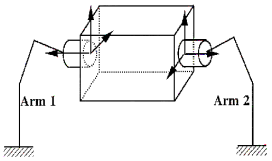

Figure 1: Dual robot coordinated control

$$\frac{\partial J}{\partial s} = 0.$$

Once the motion reference s is determined, the planner of each robot can calculate the desired inputs for the system. It can be seen that the planners driven by the event-based motion reference always give the optimal plan to minimize the coordination error.

The coordination scheme was implemented on two PUMA 560 6-DOF robot arms equipped with FSA-3254 6-Axis force/torque sensors. The planning and control algorithms were implemented in SGI 4D/340 workstation, which has four symmetric processors. Two of them were used to implement the feedback for two robots; and the third one was used to implement the motion reference and planners. The given task, as shown in Figure 1, was to transport a carton box, weighing 0.45 kg, by squeezing it. In the experiment, the box is moved in different directions by a pair of robot arms. One direction of movement is orthogonal to the direction of the squeezing force. The other direction is parallel to the squeezing force. The sampling rate for position and velocity measurements was 1000 Hz and for force/torque was 500 Hz. The feedback was computed at a rate of 1000 Hz.

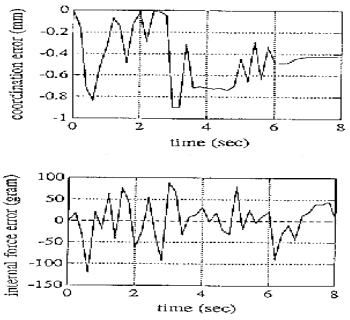

Figure 2: The motion direction orthogonal to internal force direction

The experiments have been conducted for different tasks, in which the motion direction and force control direction are either the same Figure 2 or different Figure 3. The experimental results have shown that the average coordination error is under $2mm$ and the average force control error is under $150g$ for $1000g$ commanded force. Due to the accurate control and coordination, the robot arms firmly hold the box without dropping nor breaking during the entire experiment.

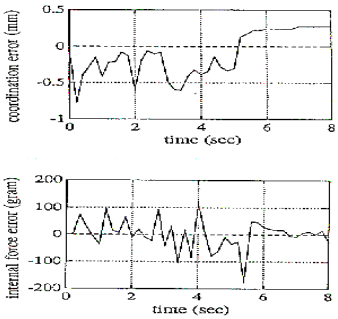

Figure 3: The motion and internal force in same direction

The experimental results have also illustrated that changing objects with different dimensions and weights does not affect the performance of the system. It clearly demonstrates that the new formation control scheme is applicable to the coordinated control of multiple manipulators.

3.3 Formation of multiple satellites

In recent years, the innovative idea of using clusters of satellites flying in formation for high-resolution, synthetic-aperture imaging has been seriously considered. An in-plane formation consists of a group of satellites occupying the same orbital plane and separated by mean anomaly. Figure 4 shows an in-plane

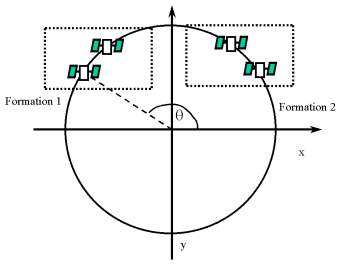

Figure 4: In-plane formations in a circular orbit

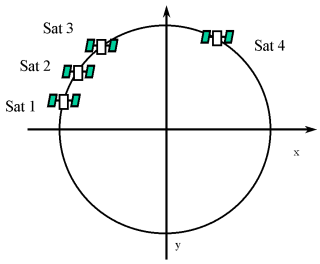

Figure 5: New formations

formation of four satellites in a circular orbit. The desired trajectory of each satellite is the circle

$$x_d = r_0 \cos(\omega t) \quad y_d = r_0 \sin(\omega t) \tag{14}$$

where r_0 is the radius of the orbit, and ω is the angular velocity. It is known that $\omega = (\frac{\mu}{r_0^3})^{1/2}$, and $\mu = 3.986 \times 10^{14}\ m^3/s^2$.

The coordinate system has inertially fixed x, y and z directions. The origin of the coordinate system is the center of the earth. The desired orbit is in the xy-plane. Following the design algorithm, the first step is to find feedbacks for each satellite to track the ideal orbit (14). In the present example, we adopt the following feedback to linearize the dynamics of a satellite.

$$\begin{aligned} &v_1 = -r\dot{\theta}^2 + \frac{\mu}{r^2} + v_1', \quad v_2 = r(\frac{2}{r}\dot{r}\dot{\theta} + v_2'), \\ &v_3 = \frac{\mu}{r^3} z + v_3', \end{aligned} \tag{15}$$

where (r, θ, z) are the cylindrical coordinates. The new control inputs v_1', v_2', v_3' are given by

$$\begin{aligned} &v_1' = a_1(r - r_0) + a_2\dot{r}, \quad v_2 = b_1(\theta - \omega t) + b_2(\dot{\theta} - \omega) \\ &v_3 = c_1 z + c_2 \dot{z}. \end{aligned} \tag{16}$$

The coefficients a_1, a_2 are determined using LQR method. Details of this feedback can be found in [3].

The action reference for the circular orbit is defined to be $s = \theta$, the angle between the radius of a satellite and the x-axis. On the desired path, $\theta = v(t) = \omega t$. The calculation of s uses a reference projection $\theta = \gamma_i(x, y)$. The definition of γ_i defines the relationship between the satellites. It determines the way that subsystems coordinate with each other.

Consider the in-plane formation of four satellites shown in Figure 4. There are two formations in the figure and each formation consists of two satellites. The satellites are supposed to keep a constant distance from each other. The value of θ_i, $1 \le i \le 4$, is defined to be the angle between the radius of the ith satellite and the x-axis, i.e., $\theta_i = tan^{-1}\frac{y_i}{x_i}$. The desired angle between the two satellites in a formation is θ_0. The feedback defined by (15)-(16) is denoted by $u(x_i, y_i, \dot{x}_i, \dot{y}_i, t)$. The reference projection of each satellite is

$$\gamma_1 = \theta_1, \quad \gamma_2 = \theta_1 - \theta_0, \quad \gamma_3 = \theta_3, \quad \gamma_4 = \theta_3 - \theta_0. \tag{17}$$

The final controller is time invariant, which is defined by $\alpha_i(x_i, y_i, \dot{x}_i, \dot{y}_i) = u(x_i, y_i, \dot{x}_i, \dot{y}_i, \frac{1}{\omega}\gamma_i), \quad i = 1, 2, 3, 4$. In this design, Sat 1 and Sat 3 are team leaders. Due to application requirement, on-line formation reconfiguration is necessary. For example, if the mission requires a new formation in which the first three satellites flying closely, the challenge is to smoothly shift sat3 closer to Sat2, while keeping Sat4 stay in its original desired trajectory (Figure 5). This can be achieved easily in our control architecture by modifying the reference projection without changing the feedback law $u(x, y, \dot{x}, \dot{y}, t)$ in (15)-(16). A new set of reference projection is defined for the reconfiguration.

$$\gamma_4 = \theta_4, \quad \gamma_3 = \theta_1 - 2\theta_0 \tag{18}$$

The term $-2\theta_0$ in the projection implies that Sat3 and Sat1 form an angle of $2\theta_0$.

In the simulation, the four satellites are flying the formation in Figure 4. The reference projection is (17). At the time $t = 5$ (days), a new formation shown in Figure 5 is to be achieved. The reference projections, γ_3 and γ_4, are switched to (18). In Figure 6, the relative angles between Sat1 and the rest of the three satellites are shown. So, the curves in the Figure 6 represent $\theta_1 - \theta_2$, $\theta_1 - \theta_3$ and $\theta_1 - \theta_4$. When $t < 5$, the formation is kept by the feedback and the reference projection (17). At $t = 5$, the projections are changed to reconfigure the formation. Under the new projections (18), the third satellite is merged to the first formation, and Sat4 stays in the second formation. In the simulation, $r_0 = 42241\ km$. In the LQR design, the weight of control is $10^{17}\frac{1}{\omega}$ ([3]). The closed-loop eigenvalues are $-0.3671(1 \pm \sqrt{-1}) \times 10^{-5}$. The distance between the two satellites in a formation is 1 km. So, $\theta_0 = 0.0013564$ degree. At the initial position, the distance between Sat1 and Sat3 is 5 km. Because of the small closed-loop eigenvalues, the mag-

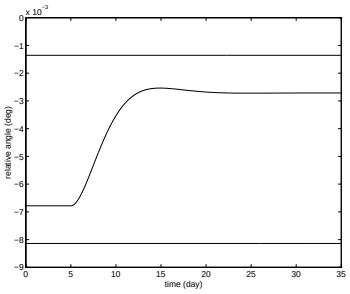

Figure 6: Formation reconfiguration

nitude of the control input is limited within the range of 10^{-9} $km/second^2$.

5 Conclusion

A general method of controller design for the formation of multiple vehicles is developed in this paper. Simulations and experiments show that the designed controllers can coordinate multiple subsystems simultaneously and drive them move in a given formation. The controller design algorithm developed in this paper has several advantages. First, the controller can follow various coordination strategies in the presence of unexpected event. Changing from one coordination strategy to another does not require major replanning. The second advantage of the algorithm is its ability of easy system reconfiguration. Adding vehicles into or removing vehicles from the formation do not require re-design of the lower level feedbacks. Furthermore, the feedbacks of the vehicles are not centralized controllers, the on-line computation can be easily carried out in a distributed computational environment. The third advantage is that feedbacks of subsystems can be designed using almost any trajectory tracking technique in the literature.

References

[1] W. Kang and N. Xi, "Non-Time referenced tracking control with application in unmanned vehicle," Proc. IFAC World Congress of Automatic Control, Beijing, China, July 5-9, 1999.

[2] T.J. Tarn, A.K. Bejczy and Ning Xi, "Intelligent Planning and Control for Robot Arms," Proceedings of the IFAC 1993 World Congress, Sydney, Australia, July 18-23, 1993.

[3] W. Kang, "Control of Multi-Satellite Systems in Formation," Technical Report, AFRL, March, 1999.

[4] C. R. McInnes, "Autonomous ring formation for a planar constellation of satellites," *J. Guid. , Contr., and Dynm.*, Vol. 18, NO. 5, pp. 1215-1217, 1995.

[5] M. Sampei, T. Tamura, T. Itoh and M. Nakamichi, *Path tracking control of trailer-like mobile robot*, IEEE/RSJ International Workshop on Intelligent Robots and Systems IROS'91, pp. 193-198, Osaka, Japan, 1991.